Arch. Metall. Mater. **71** (2026), 2, 473-480

DOI: https://doi.org/10.24425/amm.2026.158826

R.A. MALEK[1,2*], N. KAMARUDDIN[3], S.H.M. SALLEH[1,4], S.S.C. ABDULLAH[1,2], S. GOOVEN[5], B. THAVORNYUTIKARN[6]

THERMAL RESILIENCE OF ECO-BINARY MORTAR: AN EXPERIMENTAL STUDY OF HIGH-TEMPERATURE EXPOSURE

Mortar exposed to high temperatures can experience significant degradation in strength and durability. One potential solution is replacing cement with alternative pozzolanic materials, such as Rice Husk Ash (RHA), which has a high silica content when processed under controlled burning conditions. This study investigates the use of RHA as a partial replacement in mortar, with additions ranging from 5 to 20 wt.%. As the amount of RHA increased, the mortar color darkened to a grayish shade. Surprisingly, the inclusion of 5 wt.% RHA resulted in almost double the compressive strength compared to conventional mortar, while 10 and 15 wt.% additions also showed improved performance. However, the addition of 20 wt.% RHA led to a decrease in compressive strength to 12.49 MPa, below that of standard mortar. High-temperature exposure (up to 1,093°C) affected the moisture content of the cement paste, changing its appearance to a whitish-gray color and impacting its mechanical properties. The relative strength values for all samples ranged between 0.35 and 0.16. Thermal analysis showed that free water evaporated between 82 to 140°C, followed by the decomposition of Ca(OH)2 at 445 to 454°C. The results suggest that 5 wt.% RHA provides optimal properties compared to other mixtures. This study highlights that RHA, as a low-cost agricultural waste, can be effectively utilized in the mortar industry, offering an environmentally friendly solution to both waste disposal and sustainability issues.

Keywords: Rice husk ash; supplementary cementitious materials; pozzolanic materials; high temperature mortar

1. Introduction

In recent years, the construction industry has increasingly turned towards eco-friendly and sustainable materials to mitigate environmental impacts and promote resource efficiency. Among these materials, eco-binary mortars comprising a mixture of conventional binders and Supplementary Cementitious Materials (SCMs) with pozzolanic properties have gained significant attention due to their ability to reduce the carbon footprint of mortar production [1-3]. These mortars incorporate industrial by-products such as fly ash, slag, silica fume and agricultural wastes such as Rice Husk Ash (RHA), which have demonstrated favorable properties in enhancing mechanical performance, durability and thermal stability [4,5]. Among SCM candidates, it was determined that more researchers had been involved in the possibility of using RHA than other agricultural waste and other by-products. This is due to high siliceous content ranging from 85 to 95% [6] with pozzolanic or hydraulic properties in properly controlled burning conditions [6-8]. Therefore, RHA has emerged as a promising SCMs due to its high silica content and pozzolanic properties, enhancing concrete's mechanical and durability characteristics.

The production of RHA involves controlled combustion of Rice Husks (RHs), which is crucial for achieving the desired amorphous silica content and pozzolanic reactivity. Studies have shown that the combustion temperature, duration and cooling process significantly affect the quality of RHA, with optimal conditions leading to improved mortar properties such as increased compressive strength and reduced permeability [9,10]. Moreover, this activity was also highlighted as one of the efficient processes for carbon capturing during the curing process [11]. For this process, the carbonation formed due to the reaction of SCMs materials eventually transforms into stable carbonates through the enhancement of SCMs pore structure. This is beneficial to thermal conductivity and conserves energy for heating and cooling.

[1] UNIVERSITI MALAYSIA PERLIS (UNIMAP), FACULTY OF CHEMICAL ENGINEERING & TECHNOLOGY, TAMAN MUHIBBAH, 02600 JEJAWI, PERLIS, MALAYSIA
[2] CENTER OF EXCELLENT FRONTIER MATERIALS RESEARCH, 01000 SERIAB, PERLIS, MALAYSIA
[3] UNIVERSITI TEKNOLOGI MARA (UITM), SCHOOL OF REAL ESTATE AND BUILDING SURVEYING, COLLEGE OF BUILT ENVIRONMENT, SHAH ALAM, SELANGOR, 40450, MALAYSIA
[4] CENTER OF EXCELLENT GEOPOLYMER AND GREEN TECHNOLOGY, TAMAN MUHIBBAH, 02600 JEJAWI, PERLIS, MALAYSIA
[5] INFINEON TECHNOLOGIES (KULIM) SDN. BHD, INFINEON PLANT, LOT 10 & 11, JALAN HI-TECH 7, TAMAN KULIM HI-TECH, 09000 KULIM, KEDAH, MALAYSIA
[6] NATIONAL METAL AND MATERIALS TECHNOLOGY CENTER, THAILAND SCIENCE PARK, PATHUMTHANI 12120, THAILAND

* Corresponding author: rohayamalek@unimap.edu.my

To some extent, the non-beneficial use of RH to produce secondary by-products has been spotlighted as it is possible to overcome a few issues related to the environment and disposal of RH in landfills. Among these justifications, a major concern about their effect on sustaining good strength during fire exposure could be considered since using RHA in mortar or mortar would impact their properties. When exposed to high temperature, the chemical composition and physical structure of the mortar change considerably due to dehydration released by bound water of Calcium-Silicate-Hydrate (C-S-H) starting at 200°C, disintegrates Calcium Hydroxide ($Ca(OH)_2$) and C-S-H breakdown at 400-600°C. This is followed by loss of strength, durability and microstructural changes as it reaches temperature greater than 1,000°C [6,7]. RHA has been identified as an acceptable pozzolan replacement for cement in mortar. However, previous researchers have given far too little attention to using RHA as a SCM capable of resisting high temperature. Therefore, it is essential to understand if the alteration in mortar composition would affect the properties of the mortar at high temperature.

2. Materials and methods

2.1. Materials

Ordinary Portland Cement (OPC), fine aggregate, and RHA were used in this study. RHs are locally available in the northern state of Malaysia, Perlis. They are sourced from a rice milling factory known as KilangBeras BERNAS Sdn. Bhd., Simpang Ampat, Perlis, Malaysia.

2.2. Rice Husk Ash (RHA) Preparation and Characterization

RH was prepared under controlled burning conditions at 650°C for one hour with a heating rate of 10°C/min, followed by grinding and sieving processes to obtain 63 µm particle size. A detailed explanation of the effect of burning temperature and the assessment can be viewed in [12]. To determine the chemical composition of RHA, a mixture of 0.5 g of RHA with a grain size of 20 mm and 5 g of spectroflux was prepared and proceeded for ignitation at 1100°C for 20 min before it was cast into 32 mm diameter glass discs. Consequently, the sample was analyzed using fully automated PanAnalytical Axios Max (Holland) X-ray Fluorescence (XRF) with a standard elemental setup. The results are listed in TABLE 1. For the outer and inner epidermis of RHA, it was observed at high magnification up to 2000× using a JEOL JSM-6460 LA Scanning Electron Microscope (SEM) as displayed in Fig. 1. The SEM was operated at an accelerating voltage of 20 kV, and images were captured using a secondary electron detector to obtain detailed surface morphology and texture. For sample preparation, RHA was mounted on conductive carbon tape and inserted into the SEM chamber, followed by scanning the surface of the sample and generating high-resolution images that revealed the intricate details of the RHA's epidermal layers. Meanwhile, the respective X-ray diffraction (XRD) pattern was obtained from the Bruker D2 Phaser using an X-ray source of CuKα radiation (λ = 1.5406 Å) and an angular range between 10° and 70°. According to the XRD pattern, the ashes contained predominantly an amorphous silica phase due to a broad hump centered around 22° (2θ) without any appearance of sharp crystalline peaks, as illustrated in Fig. 2.

TABLE 1

The details of Perlis RHA used in the

Parameters	RHA
SiO_2 (wt.%)	88.991
Al_2O_3 (wt.%)	0.050
Fe_2O_3 (wt.%)	0.117
CaO (wt.%)	1.177
MgO (wt.%)	0.596
K_2O (wt.%)	6.499
Na_2O (wt.%)	0.048
SO_3 (wt.%)	0.713
Other (wt.%)	1.809
Mean Particle size (µm)	386.4
Specific gravity	0.360

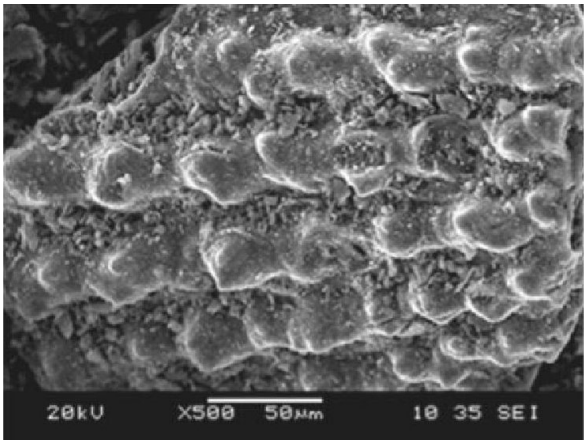

(a)

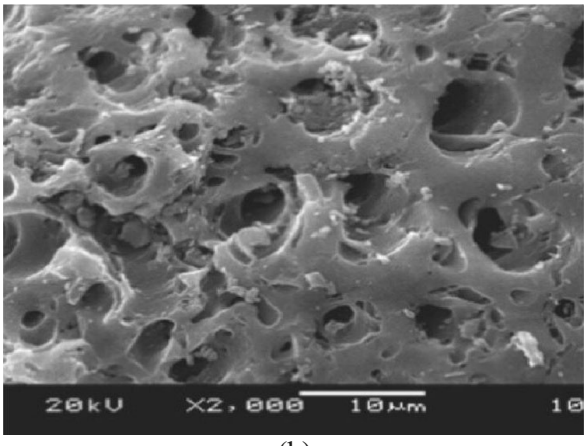

(b)

Fig. 1. The (a) outer and (b) inner parts of RHA after completing the burning process at 650°C for 1 hour duration observed using scanning electron microscopy (SEM)

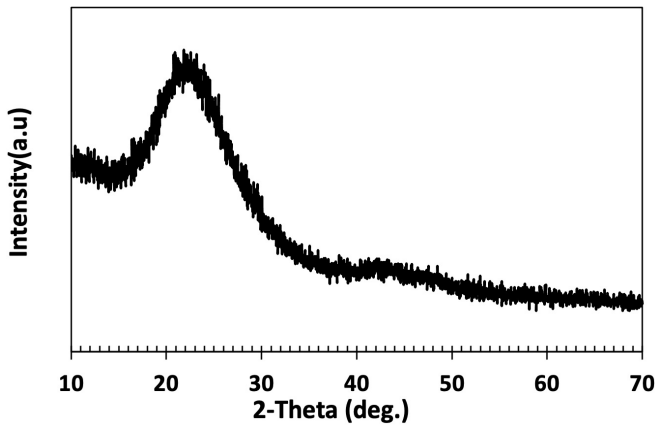

Fig. 2. XRD pattern for RHA

2.3. Mixing Procedure

The amount of RHA, OPC, fine aggregates and water required for the cube mold with a dimension of 50×50×50 mm was calculated as shown in TABLE 2. The first mixture was the control sample, while the subsequent mixtures, identified as M1 to M4, were mortar mixed with RHA at different compositions between 5% and 20% to be used for comparison. The water-to-binder (w/b) ratio demand was set at 0.4 for all mixtures. Note that all the mortar mixtures were de-molded after 24 hours and then water-cured for 28 days.

TABLE 2

Designations and mix proportions of mortar mixtures

Mixture ID	OPC (wt.%)	RHA (wt.%)	Fine Aggregate (kg/m^3)	Water (kg/m^3)
Control	100	…	544	170
M1	95	5	544	170
M2	90	10	544	170
M3	85	15	544	170
M4	80	20	544	170

2.4. Visual inspection

Visual inspection was conducted to observe the differences on mortar appearance due to the effects of high temperature exposure. The details inspections included the color changes and external mortar surface to observe any cracks or voids that might be presence.

2.5. Mass loss rate

Mass loss rate was calculated using Eq. (1) for all the tested mortars purposely to determine the effect of fire testing on the weight of the mortar samples.

$$\text{Mass loss rate (\%)} = \left(\text{Final weight} - \text{Initial weight}\right) \times 100\% \quad (1)$$

2.6. Testing on density

Density measurements were carried out using Archimedes' principles for all samples before curing, after water curing and after fire testing to understand the effect of fire on the density of the mortar. The density was calculated using Eq. (2).

$$\text{Density, } \rho = \frac{\text{Different in mass}\left(\text{g}\right)}{\text{Volume}\left(\text{m}^3\right)} \times 100 \quad (2)$$

2.7. Testing on Compressive Strength

In compliance with standard requirements, the cube specimens with dimensions of 100×100×100 mm in various curing ages between 7 and 28 days were used and have been tested before and after fire test using a compressive testing machine. The average compressive strength of the three specimens representing each of the strengths of the mixture was calculated using Eq. (3).

$$\sigma = \frac{P}{A} \quad (3)$$

Where σ represents the compressive strength in MPa, P is the maximum load of the sample in newton (N), and A is the cross-sectional area of the sample in mm^2.

2.8. Testing on Fire Resistance

The mortars were heated to 1,093°C in an electric muffle furnace following the ASTM E119. This test method provides a standard time-temperature curve to which materials and components are exposed to evaluate their resistance to fire, as presented in Fig. 3.

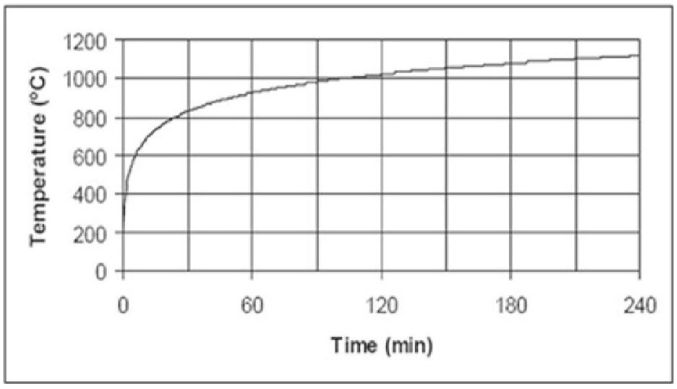

Fig. 3. Standard time-temperature curve according to ASTM E119 fire exposure

2.9. Thermal Decomposition Behaviour

A sample of pulverized powder of mortar after completing the fire test, weighing approximately 5 g, was placed in

a non-reactive pan before being placed in the TGA instrument Model TGA/DSC1 produced by Mettler Toledo instrument. The temperature was set between 25 and 1000°C under a nitrogen environment with a heating rate of 10°C/min. The system began heating the sample at the programmed rate while monitoring both weight changes.

3. Results and discussions

3.1. Visual Observation on Fire Testing

Forensic analysis by comparing the surface of mortar usually starts with visual observation of color change, cracking and spalling of mortar surface that have been conducted on all samples after exposure to high temperature. Fig. 4 portrays the mortar surfaces before and after exposure to high temperature. Note that color changes affected by high temperature can be easily identified through visual inspection. Before firing the samples, it can be seen that samples with the addition of RHA appear darker greyish compared to the control sample. This appearance occurs due to the higher carbon content in RHA as it absorps more light compared to control sample. As the amount of RHA increases, a darker greycolor will be obtained. The similar appearance also can be observed in Mosaberpanah et al. (2020) [13] work. However, discoloration occurred in all samples after the firing process was completed, resulting a final whitish-gray color. This condition was believed due to the burning off the residual carbon, other volatiles and moisture content.

As per the abovementioned findings, physical and chemical modifications were made in the heated samples. Consequently, cement paste experienced moisture evaporation, dehydration, shrinkage, or mass loss. Thermal expansion characteristics between aggregate and cement paste caused samples to crack when exposed to high temperature. A detailed investigation by Hager et al. (2014) [14] determined that water removal from the C-S-H structure is related to water-binding energy and solids. Therefore, water contained in the C-S-H structure will be eliminated starting from the evaporation of free water followed by capillary water and physically bound water. There were voids spotted on all mortar surfaces. However, long external cracking lines were visible for the control and M1 samples. As the amount of RHA increased by more than 5 wt.%, only shorter external cracking lines appeared. Surprisingly, no thermal spalling occurred that broke samples into pieces when heated up to 1,093°C for all mixtures.

3.2. Mortar Mass Loss During Fire Testing

The effect of high temperature gave variations in mass loss at different mixtures in this study. By referring to TABLE 3, two different types of mass rates were calculated. First, the mass difference after completing the curing procedure (mass rate I), and second, the mass difference after completing the heating pro-

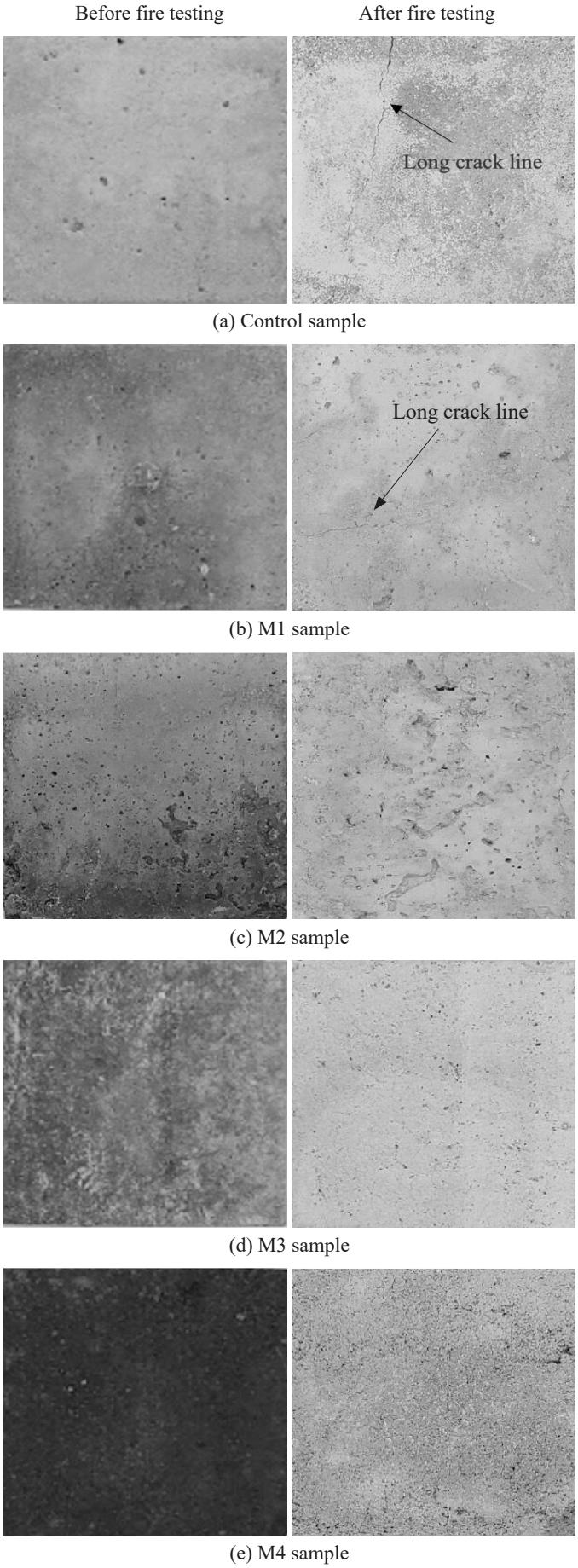

Fig. 4. Visual inspection for (a) control sample, (b) M1, (c) M2, (d) M3 and (e) M4 of RHA replacement

cedure (denoted as mass rate II). Mass rate I show no mass loss during the curing process. However, as expected, all the samples gained mass throughout the process since RHA's porous structure tends to absorb more water during the curing procedure. The sample ranging from 0 to 15 wt.% of RHA replacement showed comparable mass gain. Nonetheless, increasing the amount of RHA up to 20 wt.% has resulted in more than double the water adsorption in the C-S-H structure. Meanwhile, a similar trend in mass rate II was recorded, ranging from 4.9 to 6.3%, as all the water binds in the C-S-H structure were gradually removed during heating. To some extent, this finding fits well with the outcome of the visual observation.

TABLE 3

Calculated data of mass loss in different conditions

Mixture ID	Mass loss rate I (%)	Mass loss rate II (%)
Control Sample	0.6	5.1
M1	0.6	5.2
M2	0.6	4.9
M3	0.6	5.4
M4	1.7	6.3

The density variation in the RHA-based and conventional mortars could create a variation in compressive strength. Based on the experimental results of density, it was discovered that the control sample was denser than RHA-containing mortars. As the amount of RHA increases in mortar, a greater amount of water will be absorbed in RHA porous particles. Note that the water evaporates during heating and forms voids,contributing to less dense mortars. The density of the control sample was 2.14 gcm^{-3} and diminished to 2.10, 1.97, 198, and 1.82 gcm^{-3} for M1 to M4 samples, respectively. Consequently, these voids that are filled with air will lead to detrimental effects on their strengths.

The influence of RHA replacement on the compressive strength development of hardened mortar paste in two different conditions, namely unheated and post-heated, are presented in Fig. 5. It is evident from the results that the compressive strength of unheated samples in the control sample gave an average value

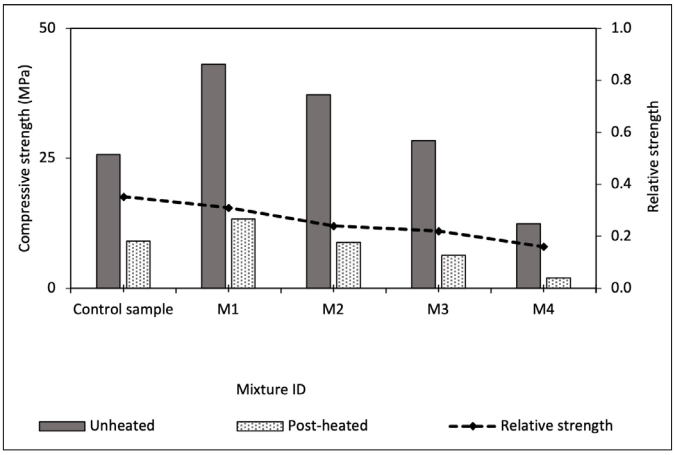

Fig. 5. Compressive strength of unheated and post-heated mortar samples at various RHA replacement amounts

of 25.73 MPa. This value is consistent with the conventional mortar made of a full mixture of OPC. Remarkably, adding RHA showed greater compressive strength values, reaching 43.10 MPa for 5 wt.% RHA addition, followed by 37.22 MPa and 28.37 MPa for 10 and 15 wt.% RHA replacement, respectively, compared to the control sample. However, the replacement of 20 wt.% showed that the mortar had drastically lost its compressive strength by more than half of the control sample. The relative compressive strength values of the mortar were recorded, ranging from 0.35 to 0.16 in parallel to the amount of RHA.

This trend is somehow related to the formation of portlandite at the early stages of the hydration reaction between cement and water. The amount of RHA replacement of up to 20% in this study seemed to affect the efficiency of silica from the RHA reacting with free portlandite [7]. Nonetheless, this study's overall unheated compressive strength result signifies that the mortar mixtures, regardless of the amount of RHA replacement, are superior for use as mortar for construction purposes.

Overall, it can be seen that the heated samples lose massive compressive strength, with losses ranging from 64% up to 88%. The ranking is M1 > Control sample > M2 > M3 > M4, respectively. The relative strength was obtained as the percentage retained strength with respect to the unheated strength. Note that the relative strength of mortar significantly decreased after high-temperature exposuresince the moisture evaporation during high-temperature exposure would have altered their mechanical properties [15,16].

All explanations for the effect of high temperature can be linked to the thermal analysis. Cement paste plays a vital role in the strength of mortar exposed to high temperatures. Consequently, all the mortar samples were tested using Thermogravimetric Analysis (TGA) to determine the reaction of the samples at elevated temperatures. The results were compared and analyzed, as presented in Fig. 6. After all the TGA patterns were compared with the control mix, it was determined that mortars containing 5% to 15% RHA had a similar pattern to the control sample. However, the sample containing 20% RHA showed an inconsistent pattern with fluctuating peaks and a mass reduction throughout the process.

For all samples, an endothermic peak corresponding to the evaporation of free water was observed. The temperatures at which this evaporation occurred varied for each sample. The evaporation stage took place earlier in the control mixture (48°C), followed by M2 (49°C) and M3 (47°C), with M1 occurring at a higher temperature (55°C). These differences in temperature indicate variations in the hydration behavior of the samples. As denoted by peak B, all samples (except M4) showed a second endothermic peak at temperatures of 82°C (control), 85°C (M1), 83°C (M2), and 140°C (M3). This suggests that water evaporation continued beyond the initial stage.

In addition, exothermic reactions were observed in all the tested samples within specific temperature ranges. The control and M1 samples exhibited a single exothermic peak at 224°C and 321°C, respectively. In contrast, the M3 and M4 samples displayed multiple exothermic peaks ranging from 118°C to

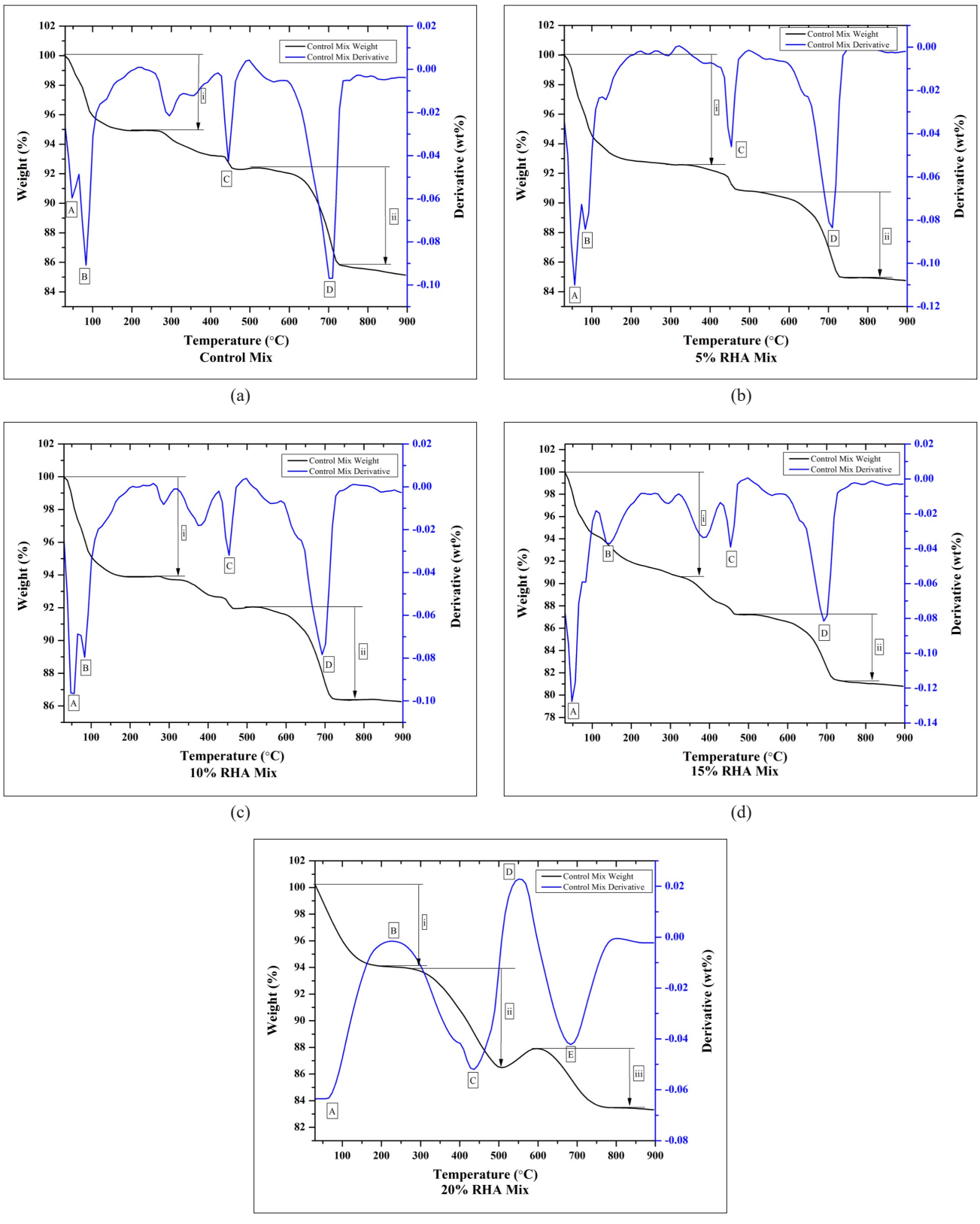

Fig. 6. TGA graphs for (a) control sample, (b) M1, (c) M2, (d) M3 and (e) M4 of RHA replacement

436°C, indicating the release of gases from these samples. Additionally, the decomposition of Calcium Hydroxide ($Ca(OH)_2$), denoted as peak C in all figures, serves as an important indicator of the thermal stability of the samples [17]. The decomposition of $Ca(OH)_2$ was observed at similar temperatures across all samples, starting with the control mix at 445°C, followed by the mortars containing RHA: M1 (5% RHA) at 455°C, M2 (10% RHA) at 454°C, and M3 (15% RHA) at 454°C [18].

The fourth endothermic peak (D) corresponds to the dehydration of C-S-H gel in the samples, which occurs at temperatures between 692°C and 710°C. This peak suggests the possible formation of new phases in the mortar due to the elevated temperature. Two different mass loss analyses were observed and marked as (i) and (ii) in the figures. Firstly, the early mass loss (i) is attributed to the evaporation of free water. The control sample shows the least mass lost with only 5%, while M1, M2, and M3 showed mass losses of 7.5%, 6%, and 10%, respectively. The second mass loss due to $CaCO_3$ Decomposition (ii) happened in the temperature range from 500°C to 850°C. The mass loss in this range was Control: 6.7%, M1 (5% RHA): 5.8%, M2 (10% RHA): 5.5% and M3 (15% RHA): 6%. The sample containing 20% RHA (M4) could not be analyzed due to its erratic behavior and lack of clear peaks in the TGA results. This might have happened due to a high silica content, which can alter the thermal properties of the sample and cause phase changes. Further investigations should be conducted to better comprehend this issue.

4. Conclusions

This paper presented an experimental investigation on the effects of mortar to high-temperature exposure with different amounts of RHA replacement. In general, this study generated an acceptable mortar property produced using RHA as SCM, which gives higher compressive strength and denser mortar since the porous structure of RHA increased the water demand in cement paste. However, exposure to high temperature revealed the color changes in the appearance of mortar from darker grayish to whitish-gray influenced by the dehydration of cement paste. The residual compressive strength was reduced by more than half of the initial value due to dehydration that altered their mechanical properties. Overall, adding 5 wt.% of RHA poses good characteristics and can be used in construction fields.

Acknowledgments

We would like to extend our appreciation for the support from the Fundamental Research Grant Scheme (FRGS) under grant number9003-00748**:** FRGS/1/2019/TK06/UNIMAP/02/6 from the Ministry of Higher Education (MoHE), Malaysia and grant number 600-RMC/MyRA 5/3/LESTARI (053/2020).

REFERENCES

[1] J. Bawab, J. Khatib, H. El-Hassan, Sustainable mortar containing supplementary cementitious materials. Sustainable Concrete Materials and Structures, p. 41 (2024). DOI: https://doi.org/10.1016/b978-0-443-15672-4.00003-6

[2] M. Hossain, R. Cai, S. Ng, D. Xuan, H. Ye, Sustainable natural pozzolana mortar – A comparative study on its environmental performance against concretes with other industrial by-products. Constr. Build. Mater. **270**, Jan. (2021). DOI: https://doi.org/10.1016/j.conbuildmat.2020.121429

[3] S. Kushwah et al., Mixture of biochar as a green additive in cement-based materials for carbon dioxide sequestration. Journal of Materials Science: Materials in Engineering **19**, 1, 27 (2024). DOI: https://doi.org/10.1186/s40712-024-00170-y

[4] M. Thiedeitz, B. Ostermaier, T. Kränkel, Rice husk ash as an additive in mortar – Contribution to microstructural, strength and durability performance. Resour. Conserv. Recycl. **184**, 106389 (2022). DOI: https://doi.org/10.1016/j.resconrec.2022.106389

[5] S. Endale, W. Taffese, D.-H. Vo, M. Yehualaw, Rice Husk Ash in Mortar. Sustainability **15**, 137, Dec. (2022). DOI: https://doi.org/10.3390/su15010137

[6] M. Amran et al., Rice husk ash-based mortar composites: A critical review of their properties and applications. Materials (2021). DOI: https://doi.org/10.3390/cryst11020168

[7] M. Thiedeitz, W. Schmidt, M. Härder, T. Kränkel, Performance of rice husk ash as supplementary cementitious material after production in the field and in the lab. Materials (2020). DOI: https://doi.org/10.3390/ma13194319

[8] L. Hu, Z. He, S. Zhang, Sustainable use of rice husk ash in cement-based materials: Environmental evaluation and performance improvement. J. Clean Prod., (2020). DOI: https://doi.org/10.1016/j.jclepro.2020.121744

[9] O.E. Babalola, P.O. Awoyera, D.H. Le, L.M. Bendezú Romero, A review of residual strength properties of normal and high strength mortar exposed to elevated temperatures: Impact of materials modification on behaviour of mortar composite. (2021). DOI: https://doi.org/10.1016/j.conbuildmat.2021.123448

[10] A. Siddika, M.A. Al Mamun, R. Alyousef, H. Mohammadhosseini, State-of-the-art-review on rice husk ash: A supplementary cementitious material in mortar. Journal of King Saud University - Engineering Sciences (2021). DOI: https://doi.org/10.1016/j.jksues.2020.10.006

[11] J. Liu, G. Liu, W. Zhang, Z. Li, F. Xing, L. Tang, Application potential analysis of biochar as a carbon capture material in cementitious composites: A review. Constr. Build. Mater. **350**, 128715, Oct. (2022). DOI: https://doi.org/10.1016/j.conbuildmat.2022.128715

[12] R. Abdul Malek, G. Subramaniam, N. Kamaruddin, S.S. Che Abdullah, Assessment on Optimal Level of Reactive Biosilica Affected by Incineration Conditions in Perlis Rice Husk Ash as Supplementary Cementitious Materials in Mortar. Key Eng. Mater. **930**, 179-186, Aug. (2022). DOI: https://doi.org/10.4028/p-qz2r64

[13] M.A. Mosaberpanah, S.A. Umar, Utilizing Rice Husk Ash as Supplement to Cementitious Materials on Performance of Ultra High Performance Mortar: – A review. Materials Today Sustainability **7-8**, 100030 (2020). DOI: https://doi.org/10.1016/j.mtsust.2019.100030

[14] I. Hager, Colour Change in Heated Mortar. Fire Technol. (2014). DOI: https://doi.org/10.1007/s10694-012-0320-7

[15] F.M. Nazri, S. Shahidan, N.K. Baharuddin, S. Beddu, B.H. Abu Bakar, Effects of heating durations on normal mortar residual

properties: Compressive strength and mass loss. In IOP Conference Series: Materials Science and Engineering (2017).
DOI: https://doi.org/10.1088/1757-899x/271/1/012013

[16] K. Selvaranjan et al., Thermal and environmental impact analysis of rice husk ash-based mortar as insulating wall plaster. Constr. Build. Mater. (2021).
DOI: https://doi.org/10.1016/j.conbuildmat.2021.122744

[17] O. Arioz, Effects of elevated temperatures on properties of mortar. Fire Saf. J. (2007).
DOI: https://doi.org/10.1016/j.firesaf.2007.01.003

[18] W.H. Wang, Y.F. Meng, D.Z. Wang, Effect of rice husk ash on high-Temperature mechanical properties and microstructure of mortar. Kemija u industriji/Journal of Chemists and Chemical Engineers (2017).
DOI: https://doi.org/10.15255/kui.2016.054